Initial nucleation site formation due to acoustic droplet vaporization

David S. Li, Oliver D. Kripfgans, Mario L. Fabiilli, J. Brian Fowlkes, and Joseph L. Bull
University of Michigan, Ann Arbor, Michigan 48109, USA

(Received 8 November 2013; accepted 2 January 2014; published online 11 February 2014)

Acoustic droplet vaporization (ADV) is the selective vaporization of liquid microdroplets using ultrasound, resulting in gas bubbles. The ADV process has been proposed as a tool in biomedical applications such as gas embolotherapy, drug delivery, and phase-change contrast agents. Using a 7.5 MHz focused transducer, the initial gas nucleus formed in perfluorocarbon microdroplets was directly visualized using ultra-high speed imaging. The experimental results of initial nucleation site location were compared to a 2D axisymmetric linear acoustic model investigating the focal spot of the acoustic wave within the microdroplets. Results suggest a wavelength to droplet diameter dependence on nucleation site formation. © *2014 AIP Publishing LLC*.
[http://dx.doi.org/10.1063/1.4864110]

Acoustic droplet vaporization (ADV) is a process in which liquid microdroplets are selectively vaporized using ultrasound to form larger gas bubbles. The ADV process has been proposed as the primary mechanism behind a potential ultrasound-based cancer therapy called gas embolotherapy (GE).[1–3] In GE, liquid perfluorocarbon (PFC) microdroplets are intravenously injected into the bloodstream to freely circulate throughout the circulatory system. The PFCs chosen for droplet formulation have a boiling point below body temperature (i.e., $<37\,^{\circ}C$) and include a lipid or albumin shell stabilizing the droplet. However, the degree of superheat of the PFC microdroplets is below the critical limit of super heat ($T_C = 148\,^{\circ}C$),[4] eliminating the possibility of spontaneous explosive boiling from occurring. Previous studies have shown that PFC microdroplets remain stable beyond $65\,^{\circ}C$.[1,5] Studies have shown that ADV can offer sufficient occlusion in a supply vessel showing promise for GE.[6,7] In addition to GE, the ADV process has been proposed as a platform for localized drug delivery,[8–10] HIFU tumor ablation,[11] and phase-change contrast agents.[12,13]

Few studies have examined the dynamics of the ADV process of PFC microdroplets. Earlier work paralleling the dynamics of ADV began with shock-induced explosive boiling by Frost in 1989.[14] Frost observed that the shock-induced vaporization process of liquid isopentane droplets differed from spontaneous explosive boiling. One of Frost's observations was that during shock-induced vaporization two consecutive gas nucleation sites developed in line with the propagation direction of the shockwave. The first nucleation site consistently appeared further from the shockwave source near the droplet interface, but never on the hemisphere proximal to the acoustic source. In the context of ADV of PFC microdroplets, Kripfgans *et al.* investigated the mechanism leading to nucleation[2] and Wong *et al.* focused on the expansion rates of PFC microbubbles following ADV.[15] Both Kripfgans *et al.* and Wong *et al.* shared similar observations with Frost that when two gas nucleation sites were formed, they were both on axis with the ultrasound. Kripfgans *et al.* hypothesized that the threshold for ADV of PFC droplets was directly linked to the amplitude in which the ultrasound was able to translate the droplet in an oscillatory fashion.[2] Giesecke and Hynynen recorded acoustic cavitation noise from ADV and hypothesized that nucleation originated outside the droplet interface as a cavitation bubble impinging on the droplet, penetrating the albumin shell, and initiating vaporization.[5] The proposed mechanism contradicted results suggesting that onset of ADV originates within the droplet and is cavitation independent.[2,16,17] More recently, Shpak *et al.* observed the nucleation process in single and double emulsion PFC droplets where in the latter case consistent localization of vaporization was observed, originating at 0.4 R away from the center of the droplet along the axis of the ultrasound, where R is the droplet radius.[18,19] The goal for this study is to directly visualize the nucleation site formation in liquid PFC microdroplets due to the ADV process and propose a potential mechanism initiating vaporization. A greater understanding behind the mechanics of the ADV process will allow the design of safer and more effective biomedical applications.

A schematic of the experimental setup is shown in Figure 1. Individual PFC microdroplets were isolated in an acrylic tank containing degassed deionized (DI) water held

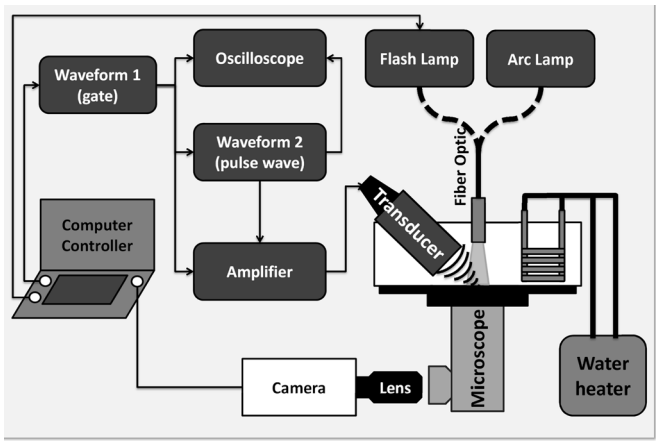

FIG. 1. Schematic of the experimental setup. The transducer and light source were oriented confocal with the inverted microscope objective. The ADV event was captured using an ultra-high speed camera through the side port of the microscope. The acoustic pulse was generated using an N cycle pulse from a function generator that was amplified prior to reaching the transducer.

at 37 °C using a temperature controlled heating coil (HTP-1500, Adroit Medical Systems, Loudon, TN). Droplets were vaporized using single pulses of 3–15 cycles at 2.2–5.1 MPa peak negative pressure (PNP) from a 7.5 MHz single element f/2 (D = 1.9 cm or 0.75 in) focused transducer (Panametrics A321S, Olympus, Waltham, MA). The transducer was fixed in place confocal to the optics at a 25° from the horizontal plane. The acoustic signal was generated by an HP 3314A function generator amplified by a Ritec GA-2500-A amplifier and monitored using an oscilloscope (WaveSurfer 44MXs, Teledyne LeCroy, Chestnut Ridge, NY). An Aligent 33120A function generator triggered the acoustic signal and gated the amplifier. The microdroplets (N = 68) featured a dodecafluoropentane liquid core (DDFP, CAS No. 678-26-2) and an albumin shell. Details on the formulation of the PFC microdroplets can be found in Kripfgans *et al.*[1] The ADV event was captured using an inverted microscope (Nikon Eclipse TE2000-S, Nikon, Melville, NY) paired with ultra-high speed camera (SIM802, Specialised Imaging Ltd, Hertfordshire, UK) with 8 discreet CCDs, which captured 16 images at a time. The optical setup included a 4×, 10×, or 20× objective with 10× internal magnification from the microscope along with a 70–300 mm Tamron f/4-5.6 macro zoom lens with a reverse mounted 50 mm f/1.4 Nikkor lens on the camera providing an additional 1.4-6× magnification. In order to provide sufficient light to image the ADV process, a 300 Joule flashlamp (Adaptec AD300, Adapt Electronics, Essex, UK) with a fiber optic bundle was used to redirect light to the field of view providing a 15 μs burst of light.

Using COMSOL (COMSOL Inc., Burlington, MA), the transient pressure acoustics module was used to simulate the acoustic field interacting with a static PFC microdroplet. The linear acoustics wave equations were solved in a cylindrical coordinate system, given by

$$\frac{1}{\rho c^2}\frac{\partial^2 p}{\partial t^2} + \nabla\left(-\frac{1}{\rho}\nabla p\right) = 0,$$

where ρ, c, p, and t represent density, speed of sound, pressure, and time, respectively. The density and speed of sound of water were assumed to be 993 kg/m^3 and 1523 m/s, respectively, while for DDFP the values were 1571 kg/m^3 and 405 m/s, respectively.[19] The model included the curved f/2 transducer element driven for 3 cycles in a water domain, a PFC droplet at the focal spot of the transducer, and the outer boundaries of the domain were radiating conditions representing unbounded constraints. The frequencies used in the study included our carrier frequency (7.5 MHz), the first harmonic (15 MHz), and the linear combination of the carrier frequency and the next two harmonics, which were matched according to intensity from hydrophone measurements (Figure 2).

Approximately 25 μs after the initial firing of ultrasound the ADV process began, which was expected considering the sound speed in degassed DI water and the focal length of the transducer. The ADV process always began with a single gas nucleation site forming within the droplet (although the transducer was oriented at a shallow angle, it is recognized that this is single directional view and thus the localization

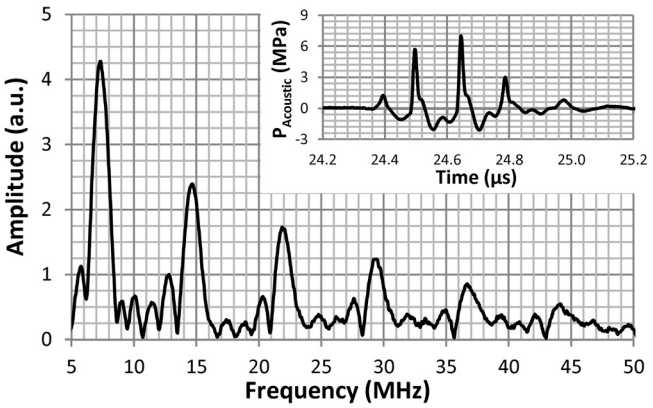

FIG. 2. Frequency response of the 7.5 MHz transducer at the focal point. The power spectrum reveals significant contribution from higher harmonics at the focus. The inset image shows the non-linear acoustic response from a 4 cycle sine input recorded from a hydrophone at the focal spot.

of the nucleation site is limited by this projection). Occasionally, a second nucleation site would form along the axis of the ultrasound propagation, which is consistent with the previous observations,[2,14] shortly after the initial nucleation site is formed. After the nuclei were formed, the liquid PFC continued converting into its gas phase causing the nuclei to grow in size. Visually, conversion of the liquid PFC to gas PFC would complete in the first 1–2 μs.

Using MATLAB, an in-house image edge detection script was used to identify and measure the distance between the centroid of the droplet and nucleus along the axis of acoustic propagation. Smaller droplets (<20 μm) had the initial nucleation site form in the hemisphere closer to the ultrasound source (Figure 3) versus initial nucleation in larger droplets (>20 μm) formed further from the ultrasound transducer. This differs from the conflicting observations from Frost[14] and Shpak *et al.*[18] who both saw initial nucleation form exclusively on opposing sides of the droplet. However, in the limit where the PFC droplets are much larger than the

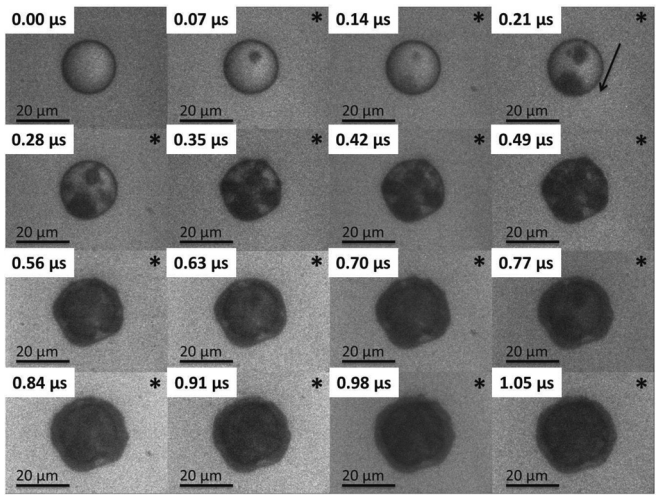

FIG. 3. An 18 μm PFC liquid microdroplet undergoing the ADV process due to a single 7.5 MHz pulse of 8 cycles at 3.6 MPa PNP. The "*" indicates the presence of the ultrasound pulse in the field of view and the arrow indicates the direction of the ultrasound wave. Note that the diameter is smaller than the carrier frequency ($\lambda = 54$ μm). The primary nucleation is formed in the second frame with secondary nucleation sites form in frames 3 and 5 (70 and 210 ns after the first nucleation side is formed).

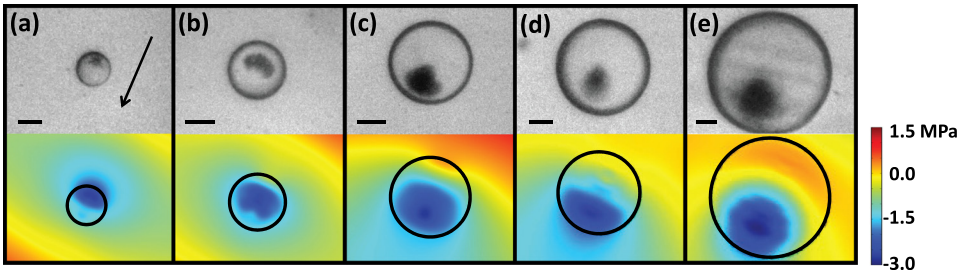

FIG. 4. Experimental results of the first nucleation site (top row) versus the simulated pressure field (bottom row) at 7.5 MHz. Image pairs (a)-(e) represent 14.2, 20.2, 28.5, 41.5, and 60.1 μm diameter droplets and corresponding results. The scale bar indicates 10 μm and the arrow indicates the direction of propagation for the ultrasound wave. The simulation results are plotted when PNP are highest when the propagating acoustic wave travels through the droplet. Blues indicate locations of negative pressure and reds represent positive pressures.

wavelength (i.e., millimeter scale), the results match Frost's in the sense that initial nucleation may appear exclusively further from the acoustic source near the boundary of the droplet. As droplet size decreased, the wavelength begins to be of similar or longer than the droplet diameter and the initial nucleus traverses across the axis of acoustic propagation and forms proximal to the acoustic source (Figure 4) matching results and conditions from Shpak *et al*. who saw nucleation form at −0.4 R.[18]

Visually, simulation results indicating the region of lowest acoustic pressure during the propagation of the acoustic wave within the droplet matched well with the experimentally observed location of first nucleation site formed (Figure 4). The simulated acoustic field shows a similar migration pattern of location of highest PNP to initial nucleus position as a function of wavelength to droplet diameter. Simulation results suggest that for droplets smaller than the half wavelength in DDFP ($\lambda = 54$ μm), the carrier frequency is unable to refocus in the droplet; thus, inclusion of harmonics better describes the location of initial nucleation for small droplets (Figure 5). This may suggest an increased reliance on higher pressures from higher harmonics for ADV of smaller droplets. Kripfgans *et al*. concluding that increasing transducer frequency lowers droplet vaporization threshold and also broadens the size range of droplets that can be easily vaporized.[2] Simulations suggest that a combination of acoustic lensing from the droplet and the short wavelength of DDFP from the slower speed of sound (405 m/s) determines where the largest PNP occurs within the droplet. However, ADV is a threshold-based process. Therefore, tracking the location of 80% of the maximum PNP would reveal sensitivity of where nucleation may occur. Simulations confirm that if the acoustic output were beyond threshold, the PNP would cross threshold sooner causing nucleation to occur closer to the transducer as a whole.

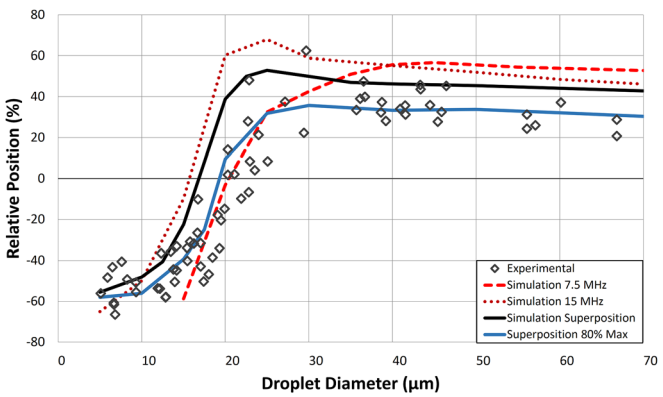

FIG. 5. The relative position of the first nucleation site in the microdroplet due to ADV versus simulated results of where the greatest PNP developed along the axis of acoustic propagation. Negative percentages indicate that the center of the first nucleation site formed closer to the transducer, while positive percentages indicate formation further from the transducer.

Mechanistically, acoustic lensing within the droplet may enhance the development of large local PNPs resulting in a cavitation-like event (i.e., nucleation site formation and onset of the ADV process). Once formed, the nucleation site appears stable and serves as a source for conversion of liquid to gaseous PFC, generating a high pressure bubble quickly undergoing rapid expansion to its equilibrium diameter described by Wong *et al*.[15]

The location and development of gas nucleation sites formed within liquid PFC microdroplets during the ADV process was imaged. Simulation results and experimental results correlate well. This suggests that due to for shorter wavelength in DDFP than in water, an acoustic refocusing may be the source of nucleation. The range of wavelength to droplet diameters tested show the transition in initial nucleation site location Frost[14] and Shpak *et al*.[18] who observed initial nuclei form on opposing sides of the droplet. For the acoustic parameters used, the results indicate that the initial gas nucleus formed is always contained within the droplets. Furthermore, the ADV mechanism directly observed is potentially a different mechanism suggested from longer pulse lengths previously proposed by Giesecke and Hynynen.[5,16,17]

This research has been funded by NIH Grant Nos. R01EB006476 and S10 RR022425.

[1]O. D. Kripfgans, J. B. Fowlkes, D. L. Miller, O. P. Eldevik, and P. L. Carson, Ultrasound Med. Biol. **26**, 1177 (2000).
[2]O. D. Kripfgans, M. L. Fabiilli, P. L. Carson, and J. B. Fowlkes, J. Acoust. Soc. Am. **116**, 272 (2004).
[3]J. L. Bull, Crit. Rev. Biomed. Eng. **33**, 299 (2005).
[4]V. Vandana, D. J. Rosenthal, and A. S. Teja, Fluid Phase Equilib. **99**, 209 (1994).
[5]T. Giesecke and K. Hynynen, Ultrasound Med. Biol. **29**, 1359 (2003).
[6]O. D. Kripfgans, C. M. Orifici, P. L. Carson, K. A. Ives, O. P. Eldevik, and B. J. Fowlkes, IEEE Trans. Ultrason. Ferroelectr. Freq. Control **52**, 1101 (2005).
[7]M. Zhang, M. L. Fabiilli, K. J. Haworth, J. B. Fowlkes, O. D. Kripfgans, W. W. Roberts, K. A. Ives, and P. L. Carson, Ultrasound Med. Biol. **36**, 1691 (2010).
[8]M. L. Fabiilli, J. A. Lee, O. D. Kripfgans, P. L. Carson, and J. B. Fowlkes, Pharm. Res. **27**, 2753 (2010).

[9]M. L. Fabiilli, K. J. Haworth, I. E. Sebastian, O. D. Kripfgans, P. L. Carson, and J. B. Fowlkes, Ultrasound Med. Biol. **36**, 1364 (2010).
[10]N. Rapoport, A. M. Kennedy, J. E. Shea, C. L. Scaife, and K. H. Nam, J. Controlled Release **153**, 4 (2011).
[11]P. Zhang and T. Porter, Ultrasound Med. Biol. **36**, 1856 (2010).
[12]P. S. Sheeran and P. A. Dayton, Curr. Pharm. Des. **18**, 2152 (2012).
[13]N. Reznik, R. Williams, and P. N. Burns, Ultrasound Med. Biol. **37**, 1271 (2011).
[14]D. L. Frost, Exp. Fluids **8**, 121 (1989).
[15]Z. Z. Wong, O. D. Kripfgans, A. Qamar, J. B. Fowlkes, and J. L. Bull, Soft Matter **7**, 4009 (2011).
[16]M. L. Fabiilli, K. J. Haworth, N. H. Fakhri, O. D. Kripfgans, P. L. Carson, and J. B. Fowlkes, IEEE Trans. Ultrason. Ferroelectr. Freq. Control **56**, 1006 (2009).
[17]O. Shpak, L. Stricker, M. Versluis, and D. Lohse, Phys. Med. Biol. **58**, 2523 (2013).
[18]O. Shpak, T. Kokhuis, Y. Luan, D. Lohse, N. de Jong, B. Fowlkes, M. Fabiilli, and M. Versluis, J. Acoust. Soc. Am. **134**, 1610 (2013).
[19]E. W. Lemmon, M. O. McLinden, and D. G. Friend, "Thermophysical properties of fluid systems," in *NIST Chemistry WebBook*, 10 February 2013.